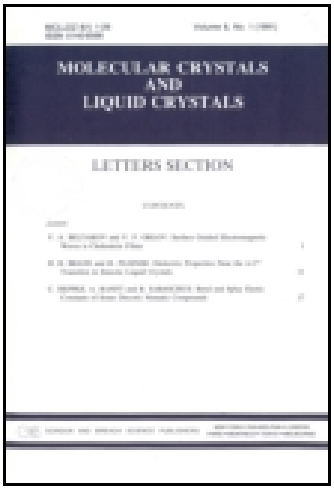

Molecular Crystals and Liquid Crystals
Publication details, including instructions for authors and subscription information:
http://www.tandfonline.com/loi/gmcl20

Quantum Dot Fluorescence in Photonic Bandgap Glassy Cholesteric Liquid Crystal Structures: Microcavity Resonance under CW-Excitation, Antibunching and Decay Time

Svetlana G. Lukishova[a], Justin M. Winkler[b] & Luke J. Bissell[c]
[a] The Institute of Optics, University of Rochester, Rochester, NY, USA
[b] Department of Physics and Astronomy, University of Rochester, Rochester, NY, USA
[c] U.S. Air Force Research Laboratory, Wright-Patterson Air Force Base, OH, USA
Published online: 30 Sep 2014.

To cite this article: Svetlana G. Lukishova, Justin M. Winkler & Luke J. Bissell (2014) Quantum Dot Fluorescence in Photonic Bandgap Glassy Cholesteric Liquid Crystal Structures: Microcavity Resonance under CW-Excitation, Antibunching and Decay Time, Molecular Crystals and Liquid Crystals, 595:1, 98-105, DOI: 10.1080/15421406.2014.917795

To link to this article: http://dx.doi.org/10.1080/15421406.2014.917795

Mol. Cryst. Liq. Cryst., Vol. 595: pp. 98–105, 2014

ISSN: 1542-1406 print/1563-5287 online
DOI: 10.1080/15421406.2014.917795

Taylor & Francis
Taylor & Francis Group

Quantum Dot Fluorescence in Photonic Bandgap Glassy Cholesteric Liquid Crystal Structures: Microcavity Resonance under CW-Excitation, Antibunching and Decay Time

SVETLANA G. LUKISHOVA,[1,*] JUSTIN M. WINKLER,[2] AND LUKE J. BISSELL[3]

[1]The Institute of Optics, University of Rochester, Rochester, NY, USA
[2]Department of Physics and Astronomy, University of Rochester, Rochester, NY, USA
[3]U.S. Air Force Research Laboratory, Wright-Patterson Air Force Base, OH, USA

Nanocrystal quantum dot (NQD) fluorescence in 1-D glassy cholesteric liquid crystal host is investigated: (1) Microcavity resonance is obtained under cw-excitation demonstrating coupling between NQD fluorescence and a cholesteric microcavity. Observed at a band edge of a photonic stopband, this resonance has circular polarization due to microcavity chirality with 4.9 times intensity enhancement in comparison with polarization of the opposite handedness. (2) Photon antibunching of a single NQD in a similar microcavity was observed. (3) Fluorescence decay time constants were measured at different excitation powers. These results are important in developing cholesteric lasers and single-photon sources for secure quantum communication.

Keywords Quantum dot fluorescence decay; lasing in cholesteric liquid crystals; microcavity resonance; antibunching

1. Introduction

One of the vibrant areas in ultrathin tunable laser development is the utilization of photonic bandgap properties of planar-aligned cholesteric (chiral nematic) liquid crystal (CLC) structures doped with dyes to create tunable compact lasers [1–10] for applications ranging from miniature medical diagnostic tools to large-area holographic laser displays [4]. Recently, liquid crystals (LC) doped with single emitters were used in polarized single-photon sources for secure quantum communication applications [11–16].

Planar-aligned CLC structures exhibit a chiral 1-D photonic bandgap for the handedness of circularly-polarized light for which the electric field vector follows the rotation of the CLC molecular director. The stop band is centered at wavelength $\lambda_0 = P(n_e + n_o)/2$, where P is the pitch of the CLC spiral structure, and n_e and n_o are the extraordinary

*Address correspondence to Dr. Svetlana G. Lukishova, The Institute of Optics, University of Rochester, 275 Hutchison Road, Wilmot building, Rochester NY 14627, USA. E-mail: sluk@lle.rochester.edu

and ordinary refractive indexes. The bandwidth of the transmission stop band is given by $\Delta\lambda \sim P(n_e - n_o)$. Lasing in such CLC structures occurs at a band edge of this stop band [2].

The photonic bandgap of CLC materials in monomeric (fluid) form can be tuned by temperature, electric and optical fields. In this paper, we use the more robust glassy oligomeric (solid) CLC form [9–15, 17, 18] as a host. Its photonic stop band can also be tuned by UV-irradiation using the change of the anisometry of the chiral-photochromic dopant [18]. In spite of the progress in development of dye-doped CLC lasers [3–7], the limitations inherent in the use of laser dyes in such compact tunable lasers are the inability of dyes to fluoresce at wavelengths of practical importance in the near-infrared, and the possibility of dye photobleaching and degradation.

Colloidal semiconductor nanocrystal quantum dots (NQDs) are more stable to bleaching than laser dyes, and some NQDs fluoresce even at telecom wavelengths 1.3 and 1.55 μm. In spite of several reports of using NQDs in different microcavities, see, e.g., references in papers [14, 19], there are only a few reports of the influence of a CLC microcavity environment on NQD fluorescence. Refs. [14–15, 18] reported circularly-polarized NQD fluorescence of definite handedness due to microcavity chirality. In our paper [20] we reported for the first time significant coupling of NQD fluorescence with a CLC photonic bandgap microcavity. We observed circularly polarized microcavity resonance (strong line narrowing) on a band edge of a photonic stop band. Recently, paper [21] reported such coupling by observing lasing in a CLC microcavity doped with NQDs at high concentration of NQDs in a monomeric CLC material.

In this paper, we describe more details of our experiment on microcavity resonance in NQD fluorescence in a photonic bandgap *glassy* CLC structure. The ability to couple emitters to a mode of a CLC microcavity suggests an application of this material to both CLC lasers and single-photon sources for secure quantum communication. We also present an experimental implementation of antibunching of NQD fluorescence in a similar glassy CLC microcavity, proving the single-photon nature of such a source. We also provide data on the dependence of NQDs' decay rates on the incident intensity in the same glassy CLC material.

2. Experimental

In our experiment, we used left-handed oligomeric cyclosiloxane CLC powder from Wacker Chemie AG (Germany) [22] doped with CdSeTe NQDs (Qdot 800 ITK organic, Invitrogen) with a fluorescence maximum, λ_0, at 790 nm. From this material, we prepared a planar-aligned glassy CLC structure with a photonic stop band centered at 910 nm for left-handed circularly-polarized light. To dope NQDs into oligomeric CLC, we heated $\sim$10 mg of the oligomeric powder on a substrate to $\sim$135°C, which is above the oligomeric's melting temperature. Then, 20 μL of NQDs dispersed in toluene were dropped into the melted oligomer and mixed with it until the solvent evaporated. The concentration of NQDs in toluene was 1 μM. The cell was prepared on a hot plate using two glass coverslips of 120 μm thickness. The coverslips were coated with polyimide and buffed. Glass spheres with 22 μm diameter defined the cell thickness. We placed NQD- doped oligomeric material on a buffed coverslip, and heated it to above the CLC oligomer clearing temperature, $T_c \sim 180$°C. The sample was then cooled to $\sim$135°C, a second coverslip was placed above the first, and the two coverslips were sheared in the direction of buffing. The oligomer was then slowly cooled to the glassy state [9–18], preserving planar-aligned CLC order (the glass-transition temperature T_g is $\sim$50°C [18]).

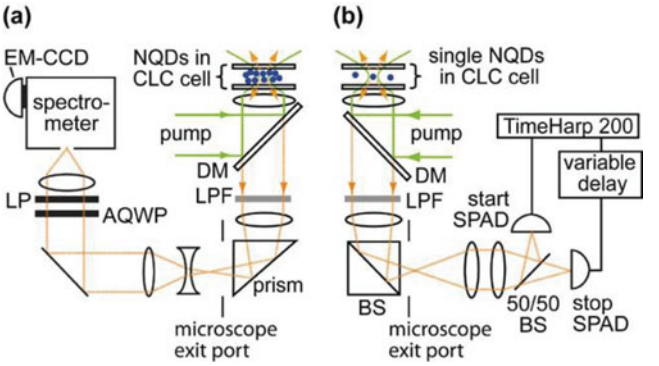

Figure 1. Schematics of experimental setup: (a) spectral and polarization measurements, (b) single-emitter confocal fluorescence imaging and photon antibunching measurements; AQWP, achromatic quarter wave plate; BS, beamsplitter; DM, dichroic mirror; LPF, long-pass interference filter set; LP, linear polarizer; SPAD, single-photon counting avalanche photodiode modules.

Figures 1 and 2 show the experimental setup for NQD fluorescence excitation and its characterization. In our measurements, we used two output ports [Fig. 1(a) and (b)] of a home-made, confocal fluorescence microscope with an oil-immersion, 1.35 NA objective to focus laser light into the CLC cell. The NQDs were excited with cw, 633-nm laser light. Fluorescence light was collected by the same objective, and interference long-pass filters provided better than 11 OD rejection of the excitation light. Figure 1(a) shows the setup used for spectral and polarization measurements. A spectrometer (SpectraPro2150i Princeton Instruments) with an EM-CCD camera (iXon DV887, Andor Technologies) was used for fluorescence spectra measurements. Circular polarization measurements were accomplished using an achromatic quarter wave plate and linear polarizer. Our polarization data were calibrated for the effect of the optical system on circularly-polarized light. We also performed a radiometric calibration of the optical system, including the spectrometer grating reflectivity dependence on polarization. In some experiments we used 532-nm, pulsed laser with 6 ps pulse duration and 76 MHz pulse repetition rate.

Figure 2. Photograph of experimental setup with one of the laser sources used in our experiments.

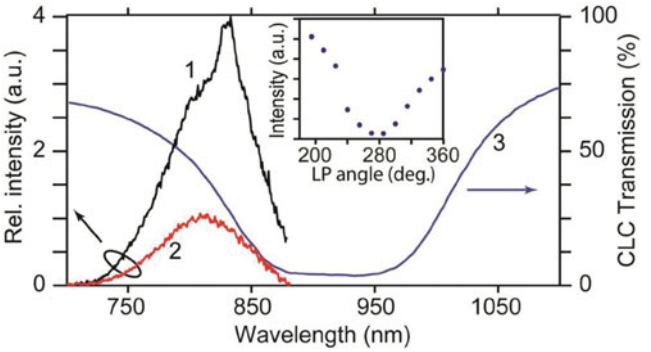

Figure 3. Circularly-polarized fluorescence resonance from CdSeTe NQDs ($\lambda_0 = 790$ nm) doped in a glassy CLC microcavity. Curve 1: LHCP fluorescence spectrum of the NQDs with a resonance at 833 nm. Curve 2: RHCP fluorescence spectrum for the same NQDs. Curve 3: selective transmission of LHCP light through a glassy CLC microcavity with a stop band centered at 910 nm (spectrophotometer measurements). Inset: Dependence of resonance peak intensity on rotation of a linear polarizer (LP) after a fixed quarter wave plate (see explanation in the text).

3. Results

Figure 3 shows the fluorescence spectra of NQDs in the photonic bandgap glassy CLC structure for two circular polarizations. Curve 1 shows the left-handed circularly-polarized (LHCP) spectrum, indicating a microcavity resonance in the NQD fluorescence. Note that the handedness of the circular polarization that experiences the photonic bandgap is the same as the circular polarization which exhibits the resonance, consistent with theory and experiments using dye as a dopant [23]. The resonance is centered at 833 nm with a FWHM of 16 nm (Q $\sim$ 50). The NQD fluorescence bandwidth without the microcavity effect was 76 nm. Curve 2 in Fig. 3 shows NQD fluorescence for right-handed circularly-polarized (RHCP) light, which does not couple to the photonic band edge mode. Curve 3 shows the transmission spectrum of the CLC structure for LHCP light, with a photonic stop band centered at 910 nm. The CLC transmission was measured with a spectrophotometer (Lambda 900, Perkin-Elmer).

The inset shows the LHCP resonance peak intensity dependence on rotation of a linear polarizer after a fixed quarter-wave plate (which was calibrated in a polarimeter). This demonstrates circularly polarized fluorescence. The NQD fluorescence diminished during the measurement, so that the intensity at the second peak in the inset is less than at the first peak. To characterize the degree of circular polarization we used the circular polarization dissymmetry factor g_e,

$$g_e = 2(I_L - I_R)/(I_L + I_R) \tag{1}$$

where I_L and I_R are intensities of LHCP and RHCP light, respectively. At the wavelength of the resonance shown in Fig. 3, g_e equals 1.3. Note that for unpolarized light, $g_e = 0$, the value which we observed with NQDs spin-coated on a bare glass slip.

The value of $I_L/I_R = 4.9$ at the resonance wavelength demonstrates intensity enhancement for LHCP light, for which there is a photonic bandgap, in contrast to RHCP light, which does not "see" it. In our measurements, the laser power on the sample was nearly 32 μW. The peak intensity in the objective focus was $\sim$23 kW/cm^2 with a focal spot diameter of $\sim$0.6 μm.

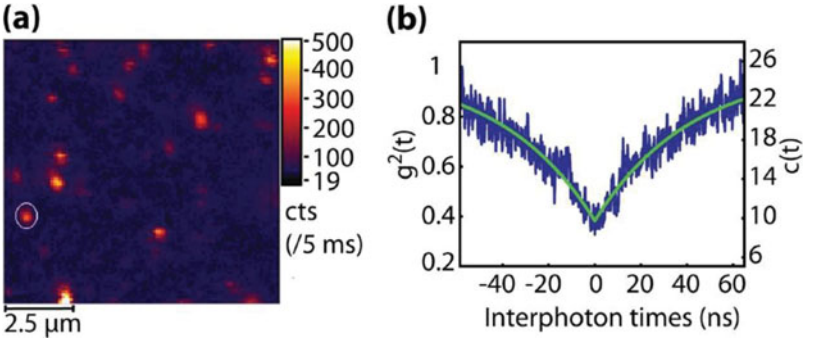

Figure 4. (a) Confocal fluorescence microscopy image of single CdSeTe NQDs ($\lambda_0 = 790$ nm) in a glassy oligomeric CLC photonic bandgap microcavity. (b) Raw coincidence counts c(t) (right-hand scale) and $g^{(2)}(t)$ (left-hand scale), showing antibunched fluorescence from a single CdSeTe NQD in this structure. Incident intensity was $\sim$1 kW/cm^2. The fitting gives decay time constant τ $\sim$41.4 ns.

To highlight the application of this glassy CLC microcavity approach to single-photon sources, we doped the same NQDs ($\lambda_0 = 790$ nm) in the same glassy Wacker cholesteric photonic bandgap structure, using an NQD concentration in toluene of $\sim$10 nM, which is two orders of magnitude less than in the previous case. The cell was again prepared from two glass coverslips with $\sim$120 μm thickness.

Antibunching with *all* photons separated in time proves the single-photon nature of the source [24–25]. In this case, the second order correlation function, $g^{(2)}(t)$, satisfies the inequality $g^{(2)}(0) < g^{(2)}(t)$. Measuring the time interval between two consecutive photons and building the histogram of coincidence counts, c(t), allows us to define $g^{(2)}(t)$, which is proportional to c(t) for sufficiently small count rates and short interphoton times [24–25]. These measurements were carried out using another port of the confocal microscope [Fig.1 (b)] by directing NQD fluorescence to a Hanbury Brown-Twiss interferometer. It consists of a beamsplitter, two single-photon counting avalanche photodiode modules (AQR-14, Perkin-Elmer), and a time-correlated single-photon counting card (TimeHarp 200, Pico-Quant) with start and stop channels. We used a 63 ns delay in the stop channel.

Figure 4(a) shows a confocal fluorescence microscope raster-scan image of single NQDs in the photonic bandgap glassy CLC structure. The laser intensity in the objective

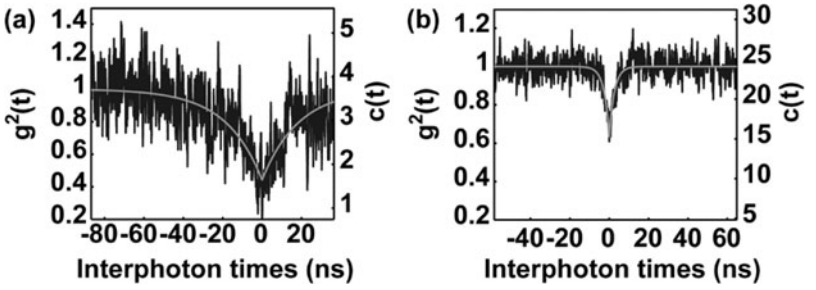

Figure 5. Raw coincidence counts c(t) (right-hand scale) and $g^{(2)}(t)$ (left-hand scale), showing antibunched fluorescence from a single CdSeTe NQD in a glassy oligomeric CLC photonic bandgap microcavity at incident intensities 1.5 kW/cm^2 (a) and 3kW/cm^2 (b). The fitting gives decay time constants $\tau \sim 18$ ns (a) and $\tau \sim 2.6$ ns (b).

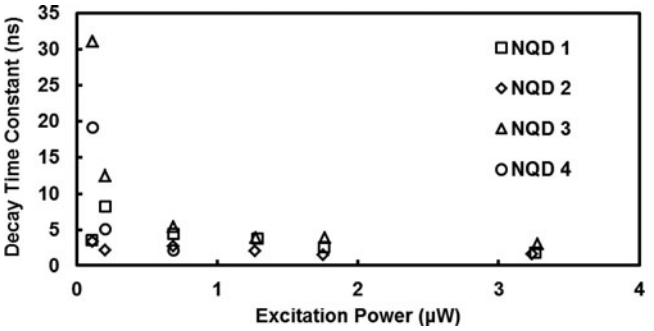

Figure 6. Dependence of NQD decay time constant on excitation power for four NQDs in glassy CLCs. For these experiments, we used a pulsed, 532-nm laser with 6 ps pulse duration and 76 MHz pulse repetition rate.

focus was ∼1 kW/cm^2, below the saturation intensity, I_{sat}. For antibunching measurements, laser light was focused into the single NQD marked by the white circle [Fig. 4(a)]. Figure 4(b) presents the coincidence histogram of this NQD fluorescence. The left–hand scale represents $g^{(2)}(t)$, which was calculated by normalizing c(t) (integrated over ∼8 min.) to the coincidence counts of a Poissonian source with the same counting rate on each detector as for our source [24–25].

The fitted value of $g^{(2)}(0)$ is 0.382 ± 0.037, indicating photon antibunching (since $g^{(2)}(0) < 0.5$, there is only one emitter). A fitting similar to that of Refs. [24–25] gives the $g^{(2)}(t)$ decay time constant $\tau \sim 41.4$ ns of this NQD. Below I_{sat} the fluorescence lifetime is approximately given by τ. Fluorescence decay curves of NQDs can be multiexponential [26–27]. Our estimate of τ for different NQDs in this sample varied, but this value corresponds to the mean value of τ for this intensity. At higher intensities, antibunching curves give a shorter τ and higher values of $g^{(2)}(0)$ due to the increased pumping rate, and also probably because of Auger-assisted nonradiative processes [26] (See Figs. 5 and 6). Importantly, our experiment proves NQD fluorescence antibunching in a glassy CLC. Our EM-CCD camera did not permit reliable observation of the resonances in the fluorescence spectrum of a *single* NQD in *the near-infrared.*

Figure 5(a, b) shows antibunching histograms for NQDs at 1.5 (a) and 3 (b) times higher incident intensities than was used for histogram of Fig. 4(b). Decay time constants obtained from these histograms are 18 ns (a) and 2.6 ns (b). Paper [28] also reports on the influence of incident light intensity on fluorescence decay rates.

We also measured fluorescence decay rates of NQDs under *pulsed* laser excitation using the same time-correlated single-photon counting card as in antibunching experiments under *cw-excitation*, but with a stop channel triggered from the laser. Figure 6 shows the dependence of NQD decay rate on incident power for four NQDs in a glassy CLC structure under pulsed, 6 ps, 76 MHz pulse repetition rate, 532-nm excitation.

4. Conclusion

In summary, we have demonstrated coupling of nanocrystal quantum dot fluorescence to the photonic band edge mode of a glassy chiral photonic bandgap CLC microcavity. In particular, we observed a circularly-polarized microcavity resonance with a bandwidth of 16 nm and a Q of ∼50 under cw-excitation [20]. These results were obtained under

cw-excitation, providing the way to cw-lasing of NQDs in CLC structures. It should be mentioned that for *dye-doped* CLCs fluorescence peaks at a band edge and even lasing under cw-excitation were reported in Refs. [23, 29]. This method can easily be extended to single-quantum-dot-doped glassy CLC structures for use as a room temperature single-photon source. Quantum dot fluorescence antibunching in such a CLC structure shows the single-photon nature of the source. The advantages of planar CLC structures over other photonic bandgap materials are the ease of preparation using well-developed LC technology and the possibility of tuning or switching the bandgap [30–33].

Acknowledgments

We thank K. Marshall for access to the LC clean room of the Laboratory for Laser Energetics. This work was supported by the NSF (ECS-0420888, EHR-0633621 and EHR-0920500). L.B. was supported by the DoD SMART fellowship. J.W. is supported by a NASA STR fellowship.

References

[1] Il'chishin, I., Tikhonov, E., Tishchenko, V., & Shpak, M. (1978). *JETP Lett.*, *32*, 24–27.
[2] Kopp, V. I., Fan, B., Vithana, H. K. M., & Genack, A. Z. (1998). *Opt. Lett.*, *23*, 1707–1709.
[3] Palffy-Muhoray, P., Cao, W., Moreira, M., Taheri, B., & Munoz, A. (2006). *Philos. Transact. A Math. Phys. Eng. Sci.*, *364*, 2747–2761.
[4] Coles, H., & Morris, S. (2010). *Nature Photonics*., *4*, 676–685.
[5] Blinov, L. M., & Bartolino, R. (2010). *Eds, Liquid Crystal Microlasers*.
[6] Chilaya, G., Chanishvili, A., Petriashvili, G., Barberi, R., De Santo M. P., & Matranga, M. A., (2011). *Scient. Research, Mater. Sci. and Appl.* ,*2*, 116.
[7] Coles, H. J., Morris, S. M., Ford, A. D., Hunds, P. J. W., & Wilkinson, T. D. (2009). *Proceed. SPIE 7414, is. 1*, 741402–1.
[8] Dolgaleva, K., Wei, S. K. H., Lukishova, S. G., Chen, S-H., Schwertz, K., & Boyd, R. W. (2008). *JOSA B 25*, 1496–1504.
[9] Shibaev, P. V., Kopp, V. I., Genack, A. Z., & Hanelt, E. (2003). *Liq. Cryst.*, *30*, 1391.
[10] Wei, S. K. H., Chen, S. H., Dolgaleva, K., Lukishova, S. G., & Boyd, R. W. (2009). *APL 94*, 041111.
[11] Lukishova, S. G., Schmid, A. W., McNamara, A. J., Boyd, R. W., & Stroud, C. R. (2003). *IEEE J. Sel. Top. Quant. Electron.*, *9*, No 6, 1512–1518.
[12] Lukishova, S. G., Schmid, A. W., Supranowitz, C. M., Lippa, N., McNamara, A. J., Boyd, R. W., & Stroud, C. R. (2004). *J. Mod. Opt.*, *51*, No 9–10, 1535–1547.
[13] Lukishova, S. G., Schmid, A. W., Knox, R. P., Freivald, P., McNamara, A., Boyd, R. W., Stroud, C. R., & Marshall, K. L. (2006). *Molec. Cryst. Liq. Cryst.*, *454*, 403–416. (See also *454*, 1–14.)
[14] Lukishova, S. G., Bissell, L. J., Menon, V. M., Valappil, N., Hahn, M. A., Evans, C. M., Zimmerman, B., Krauss, T. D., Stroud, C. R., & Boyd, R. W. (2009). *J. Mod. Opt.*, *56*, is 2 & 3, 167–174.
[15] Lukishova, S. G., Bissell, L. J., Stroud, C. R., & Boyd, R. W. (2010). *Opt. and Spectr.*, *108*, No 3, 417–424.
[16] Lukishova, S. G., & Schmid, A. W., Knox, R., Freivald, P., Bissell, L., Boyd, R. W., Stroud, C. R., & Marshall, K. L. (2007). *J. Mod. Opt.*, *54*, iss. 2 & 3, 417–429.
[17] Lukishova, & S. G., Schmid, A. W. (2006). *Molec. Cryst. Liq. Cryst.*, *454*, 15–21.
[18] Bobrovsky, A., Mochalov, K., Oleinikov, V., & Shibaev, V. (2011). *Liq. Cryst.*, *38*, 737–742.
[19] Menon, V. M., Luberto, M., Valappil, N. V., & Chatterjee, S. (2008). *Opt. Expr.*, *16*, 19535.
[20] Lukishova, S. G., Bissell, L. J., Winkler, J., & Stroud, C. R. (2012). *Opt. Lett.*, *37*, Issue 7, 1259–1261.

[21] Chen, L.-J., Lin, J.-D., Huang, S.-Y., Mo, T.-S., & Lee, C.-R. (2013). *Adv. Opt. Mat.*, *1*, N 9, 637–643.
[22] Bunning, T. J., & Kreuzer, F.-H. (1995). *Trends in Polym. Sci.*, *3* (10), 318–323.
[23] Schmidtke, J., & Stille, W. (2003). *Eur. Phys. J. B.*, *31*, 179–194.
[24] Treussart, F., Clouqueur, A., Grossman, C., & Roch, J.-F. (2001). *Opt. Lett.*, *26*, 1504–1506.
[25] Messin, G., Hermier, J. P., Giacobino, E., Desbiolles, P., & Dahan, M. (2001). *Opt. Lett.*, *26*, 1891–1893.
[26] Schlegel, G., Bohnenberger, J., Potapova, I., & Mews, A. (2002). *Phys. Rev. Lett.*, *88*, N 13, 137401–1–4.
[27] Kraus, R. M., Lagoudakis, P. G., Mu1ller, J., Rogach, A. L., Lupton, J. M., Feldmann, J., Talapin, D. V., & Weller, H. (2005). *J. Phys. Chem B, Letters*, *109*, 18214–18217.
[28] Yeh. Y.-C., Yuan, C.-T., Kang, C.-C., Chou, P-.T., & Tang, J. (2008). *Appl. Phys. Lett.*, *93*, 223110.
[29] Muñoz, A., McConney, M. E., Kosa, T., Luchette, P., Sukhomlinova, L., White, T.J., Bunning, T. J., & Taheri, B. (2012). *Opt. Lett.*, *37*, Issue 14, 2904–2906.
[30] Bobrovsky, A., Mochalov, K., Oleinikov, V., Sukhanova, A., Prudnikau, A., Artemyev, M., Shibaev, V., & Nabiev, I. (2012). *Advanced Mater.*, *24*, Issue 46, 6216–6222.
[31] Hrozhyk, U. A., Serak, S. V., Tabiryan, N. V., White, T. J., & Bunning, T. J. (2011). *Opt. Mater. Express 1*, Issue 5, 943–952.
[32] Lukishova, S. G. (2012). *Mol. Cryst. Liq. Cryst.*, *559*, 127–157.
[33] Lukishova, S. G. (2000). *J. Nonl. Opt. Phys. & Mater.*, *9*, is. 3, 365–411.